Available online at www.sciencedirect.com
SCIENCE DIRECT®
Journal of the European Ceramic Society 25 (2005) 2805–2808
www.elsevier.com/locate/jeurceramsoc

Monte Carlo simulation of the secondary electron yield of an insulating target bombarded by a defocused primary electron beam

R. Renoud [a,*], F. Mady [a], J. Bigarré [b], J.-P. Ganachaud [a]

[a] *IREENA (EA 1770), Faculté des Sciences de Nantes, 2 rue de la Houssinière, BP 92208, 44322 Nantes Cedex 03, France*
[b] *CEA-Le Ripault, BP 16, 37260 Monts, France*

Available online 5 April 2005

Abstract

We study the charge of an insulating target irradiated by a broad electron beam of a few keV with our Monte Carlo simulation model. We are particularly interested in the dynamics which leads the system towards a stationary state. We examine successively the role of parameters such as the density of current in the primary beam, the density of traps, their activation energy. According to the situation considered, one observes that the regulation of the system can sometimes be stopped, either because the traps become saturated, or, in the case of thin targets, by the appearance of a leakage current towards the ground, due to carriers released from the traps.

Keywords: Insulators; Electron microscopy; Charging effects; Defects

1. Introduction

The aim of this paper is to characterise the behaviour of an insulator bombarded by an electron beam with an energy of a few keV. We are interested more particularly in the evolution of the secondary electron emission yield $\sigma(t)$ and of the surface potential $V_s(t)$ as the system charges. The dynamics of these processes is controlled by the traps present in the sample. We make use for that of a Monte Carlo simulation model[1–3] which is well adapted to follow the history of all the charges in interaction with the sample. We have restricted our study to the case of a broad primary electron beam (defocused mode) so that the problem can be described by using a simplified one-dimensional model. The internal field and the surface potential are thus determined self-consistently, within a formalism close to that proposed by Cazaux.[4] The presence of the insulator–vacuum and of the sample–substrate interfaces is accounted for by the image charge method.[5]

2. General evolution of the system

When the primary beam energy E_p is sufficiently high, the initial total secondary emission yield σ_0 is lower than 1. One expects that the effective energy of the primary electrons, E_{eff}, will decrease during the implantation. More precisely, one predicts that $\sigma(t)$ increases progressively with the time of bombardment t to the limit $\sigma_\infty = 1$ and that the surface potential $V_s(t)$ decreases before it reaches a limit value denoted by V_∞ in what follows. One generally considers that the systems has stabilised when it is characterised by $V_s(t) = V_\infty$ and $\sigma(t) = \sigma_\infty$.

Let us first assume that the parameters characterising the system are such that no "internal constraint" restrains the evolution of the system towards a stationary state. For this, one selects a very high value for the density of trapping sites ($N_t = 10^{20}$ cm^{-3}), as well as for the activation energy of the traps ($E_a = 1$ eV) so that no detrapping effect can occur. The electric field necessary to obtain a lowering of the potential barrier of the order of E_a is about 20 MV cm^{-1}. This value, which anyway exceeds the breakdown voltage, is never attained in our calculations. The bombarded surface is fixed very large, with a primary beam radius $\phi/2 = 100$ μm.

* Corresponding author. Tel.: +33 2 51 12 55 36; fax: +33 2 40 14 09 87.
E-mail address: raphael.renoud@physique.univ-nantes.fr (R. Renoud).

0955-2219/$ – see front matter © 2005 Elsevier Ltd. All rights reserved.
doi:10.1016/j.jeurceramsoc.2005.03.144

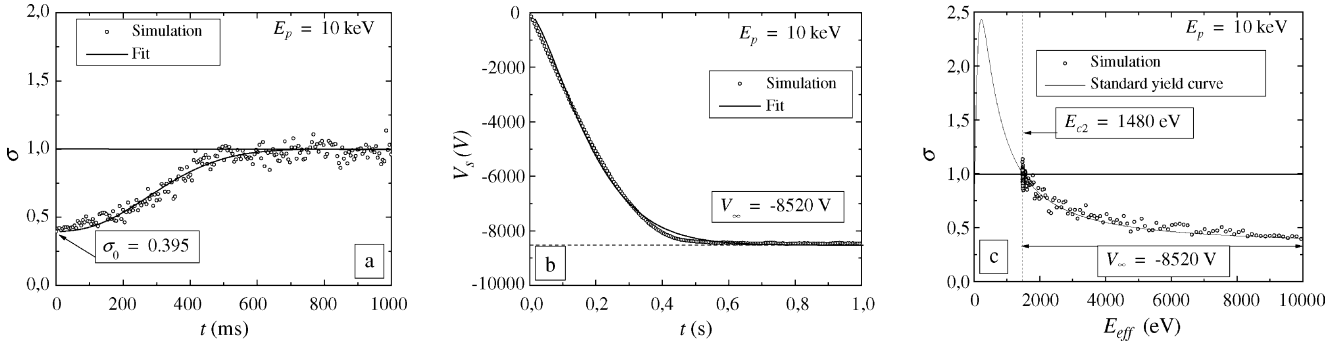

Fig. 1. Time evolution of the (a) total secondary yield σ, (b) surface potential V_s. (c) Evolution of σ as a function of the effective energy E_{eff}.

We first present the evolution of the surface potential V_s (Fig. 1a) and of the total secondary emission yield σ (Fig. 1b) as a function of the irradiation time, for $E_p = 10$ keV. The behaviours obtained by simulation are quite in conformity with those expected. In order to quantify the time evolution of V_s and of σ, we have fitted them by two sigmoidal functions:

$$V_s(t) = V_\infty \left(1 - \exp\left[-\left(\frac{t}{\tau_V}\right)^\alpha\right]\right), \quad \sigma(t) = \sigma_\infty - (\sigma_\infty - \sigma_0)\exp\left[-\frac{t}{\tau_\sigma}^\beta\right].$$

On Fig. 1c, we have reported the evolution of the total secondary emission yield, σ, as a function of E_{eff}, for the value $E_p = 10$ keV. As a comparison, we have added the yield curve obtained by assuming that all the charge effects have been inhibited ("standard" yield curve). One notices that the in-charge yield follows the standard curve perfectly. This behaviour is reproduced at all primary energies E_p. This indicates that the internal field is not sufficiently high to modify in a substantial way the trajectories of the carriers in the sample. We indeed showed recently that, in the case of a very high internal field, the in-charge yield curve $\sigma(E_{eff})$ passes above the standard one.[3] Here, σ is only affected by the surface potential effects through the modification of the beam effective energy ($E_{eff} = E_p + |e|V_s$). At the end of the charge, E_{eff} reaches the cut-off value E_{c2}, for which the yield without charge equals 1 ($E_{c2} = 1480$ eV in our example). Thus, the surface potential at stabilisation is $V_\infty = (E_p - E_{c2})/|e|$, that is $V_\infty = -8520$ V for $E_p = 10$ keV (Fig. 1c).

3. Role of the density of current

Several experiments, performed by Blaise to measure the in-charge secondary emission yield[6] show that the current density, j_0, of the primary beam plays an important role in the charge dynamics. One observes for instance that the self-regulation regime of the yield that we have described here-above is replaced by an ageing regime and then by a breakdown one when j_0 is raised. The yield or the sample current present sharp variations which accompanied by damage in the material. The current density can be modified either by varying the primary intensity I_0 or by changing the beam diameter ϕ. In the first case, and for usual intensity values, it is just necessary to adjust the time scale to account for the new irradiation rate of the primary electrons onto the target. In the second case, considered by Blaise, an electrostatic approach makes it possible to confirm the intuitive idea that the field effects are all the more marked that the diameter of the primary beam is low.[4]

We have reported on Fig. 2a the evolution of the surface potential during the irradiation for densities of current j_0 of 10^4 and 10^6 pA cm^{-2}. The regulation takes place more quickly when the density of current is increased. Of course, a reduc-

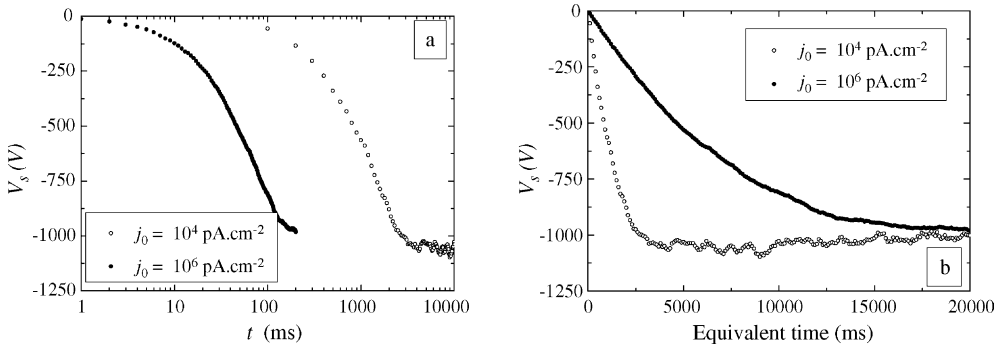

Fig. 2. Surface potential evolution $V_s(t)$ for two values of the density of current j_0: (a) real time scale, and (b) after adjustment of the time scales.

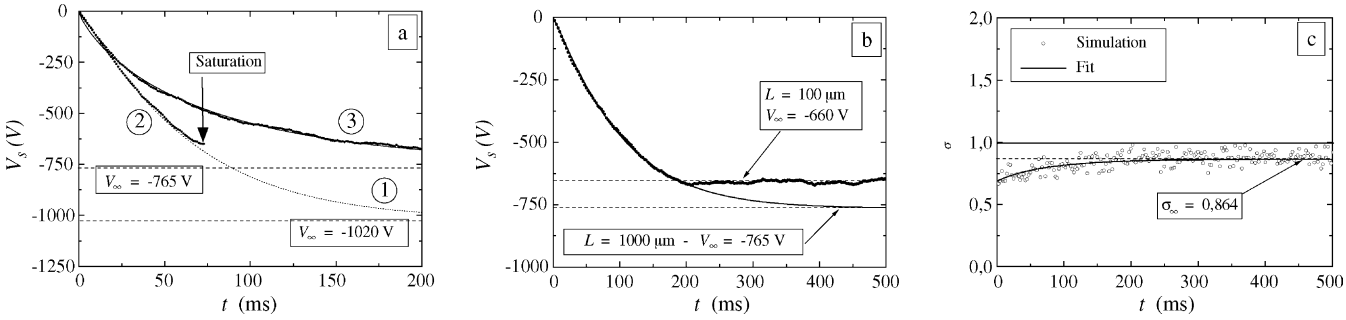

Fig. 3. Evolution of $V_s(t)$ (a) influence of the traps characteristic, (b) for two target thicknesses. (c) Evolution of the yield $\sigma(t)$ for $L = 100$ μm.

tion of the primary beam diameter ϕ is such that the charge distribution has a lesser extension at the surface. So, for a given irradiation time (same injected dose), the surface potential grows as j_0 increases. If one adjusts the time scales of time in order to recover identical current densities, one obtains the curves presented in Fig. 2b. The fact that they differ markedly indicates that the explanation is not only an effect due to the potential, but that the size of the primary spot is also a significant parameter.

The experimental results of Blaise can thus be explained by saying that, if the density of current is very high, an injected charge will not have enough time to trap before the arrival of the next primary electron at the surface of the sample. Under these conditions, an accumulation of moving charges occurs locally, eventually conferring a quasi conducting behaviour (see[7] for instance) to the corresponding region of the material (not accounted for in the present model).

4. Trapping and detrapping effects

We are now interested in the influence of the detrapping effects on the evolution of the charge within the insulating target. We consider successively samples presenting neutral traps with an either low (0.25 eV) or high (1 eV) activation energy E_a.

Our simulations indicate that, when the density of traps is high ($N_t = 10^{20}$ cm^{-3}), no noticeable differences occur in the behaviour as E_a is varied. Indeed, there are always available places for carrier trapping and the field value at stabilisation is always sensibly the same in each case. For $E_p = 2.5$ keV, The surface potential at the impact zone $V_s(t)$ varies according to the behaviour described previously (Fig. 3a, curve 1). One notably obtains a stabilisation value $V_\infty = -1020$ V.

When the density of traps is reduced ($N_t = 10^{18}$ cm^{-3}), the charge dynamics is different according to whether E_a is weak or high. When the traps are deep, the charges will occupy the same site for a long time and the "interaction pear" region can become rapidly saturated. The self-regulation of the system is then stopped before the stationary state is reached (Fig. 3a, curve 2). If on the other hand E_a is weak, the saturation effects will be less marked because of the reduction of the residence time of the carriers in the sites, resulting in a high effective mobility. The charges will be able to migrate towards regions deeper in the target. Globally, the internal field will vary slowly, just like the surface potential (Fig. 3a, curve 3). The final value reached at stabilisation is it-also reduced and one has in this case $V_\infty = -765$ V.

The effect of the migration of charges by multiple trapping can be evidenced if one works with a sample characterised by a small thickness L. In what follows, one goes from $L = 1000$ to 100 μm. Fig. 3b shows the evolution of the surface potential for $L = 100$ μm. This latter does not attain its limit value, i.e. −765 V at 2.5 keV, any more but stabilises abruptly at −660 after a time $t = 230$ ms. As well, the yield $\sigma(t)$ has now the limit value $\sigma_\infty = 0.86 \neq 1$ (Fig. 3c).

The total implanted charge and the centre of gravity of the charge stabilise more rapidly than expected (Fig. 4a). This

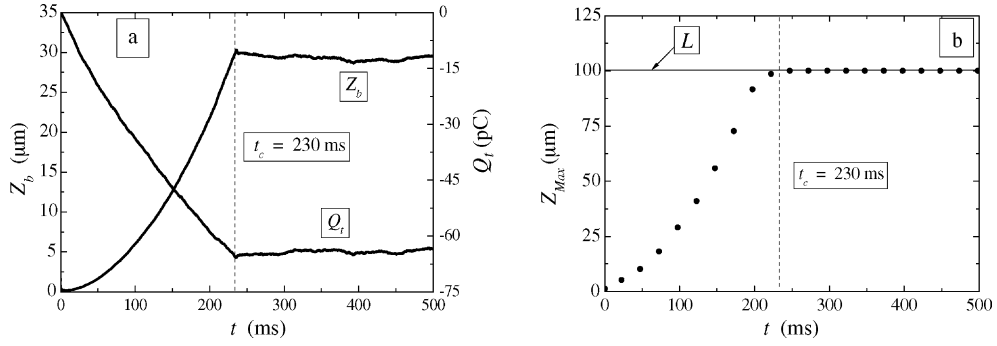

Fig. 4. (a) Evolution of the total implanted charge Q_t and of the centre of charge position Z_b for a thin target. (b) Evolution of the maximum depth of the charges Z_{Max} during the irradiation.

can only occur by a leaking of charges. Here, the only possibility is that some electrons have crossed the target and have been collected at the ground of the sample holder. Under the influence of detrapping, the maximum depth Z_{Max} attained by the charge distribution increases with the irradiation time (Fig. 4b). For $t > 230$ ms, the crossing has been achieved. This effect has recently been observed experimentally by Braga.[8]

5. Conclusion

In this study we have tried to clarify the role of the various parameters which influence the dynamics of the regulation of the charging system in the case of a broad primary beam. The nature of the traps present in the sample, their volume density as well as their activation energy are determinant. Apart from effects simply related to the penetration of the beam, the intensity of the internal field depends also on the size of the primary spot. The evolution of the charge is then governed by a competition between the filling of the traps and their relaxation under the internal field influence. According to the relative importance of the processes, different behaviours can be obtained. The "ordinary" self-regulation of the system corresponds to the case where the yield can tend continuously towards the unit. Saturation effects can also occur and stop the evolution of the yield before the above limit has been reached. At last, for a thin sample, a relaxation current to the ground can also appear, prematurely stopping the evolution of the yield.

References

1. Ganachaud, J.-P., Attard, C. and Renoud, R., Study of the space charge induced by an electron beam in an insulating target. *Phys. Status Solidi (b)*, 1997, **199**, 175–184.
2. Renoud, R., Mady, F. and Ganachaud, J.-P., Monte Carlo simulation of the charge distribution induced by a high energy electron beam in an insulating target. *J. Phys.: Cond. Mat.*, 2002, **14**, 231–247.
3. Renoud, R., Mady, F., Attard, C., Bigarré, J. and Ganachaud, J. -P., Secondary electron emission of an insulating target induced by a well-focused electron beam. Monte Carlo study. *Phys. Status Solidi (a)*, 2004, **201**, 2119–2133.
4. Cazaux, J., Some considerations on the electric field induced in insulators by electron bombardment. *J. Appl. Phys.*, 1986, **59**, 1418–1430.
5. Durand, E., Electrostatique. III. Méthodes de calcul. *Diélectriques, Masson*, 1964, 229–233.
6. Blaise, G., Charge dynamics of insulators under electron beam. In *Proceeding of the CSC'4 Conference*, 2001, pp. 31–36.
7. Ying, M. H. and Thong, J. T. L., Insulator charging under irradiation with a stationary electron probe. *Meas. Sci. Technol.*, 1994, **5**, 1089–1095.
8. Braga, D., *Etude des phénomènes de charge des matériaux isolants sous faisceau d'électrons de basse énergie* (200 eV–30 keV). Ph.D. thesis, Université Paris XI, 2003.